

Photoinduced sp^3 Nanosize Domain with Frozen Shear Displacement in Graphite

K. NISHIOKA^a AND K. NASU^b

^aInstitute for Molecular Science, Okazaki, Aichi 444-8585, Japan

^bSolid State Theory Division, Institute of Materials Structure Science

High Energy Accelerator Research Organization (KEK), Tsukuba, Ibaraki, 305-0801, Japan

A novel sp^3 -bonded nanosize domain, known as a diaphite which is an intermediate state between a graphite and a diamond, is generated by the irradiation of visible laser pulse onto a graphite crystal. The sp^3 structure is well stabilized by shear displacement between neighboring graphite layers. We theoretically study the interlayer sp^3 bond formation with frozen shear displacement in a graphite crystal, using a classical molecular dynamics and a semi-empirical Brenner potential. We show that a pulse excitation under the fluctuation of shearing motion of carbons in an initial state can generate interlayer sp^3 bonds which freeze the shear, though no frozen shear appears if there is no fluctuation initially. Moreover, we investigate a pulse excitation under the coherent shearing motion and consequently obtain that the sp^3 -bonded domain with frozen shear is efficiently formed. We conclude that the initial shear is important for the photoinduced sp^3 nanosize domain formation.

PACS: 64.70.Nd, 61.48.Gh, 31.15.xv, 05.40.-a

1. Introduction

A phase transition from a sp^2 -bonded graphite to a sp^3 -bonded diamond has been studied both theoretically and experimentally [1–8]. Generally, the diamond is synthesized macroscopically from the graphite under high temperature and pressure (3000 °C and 15 GPa, respectively) [5, 6], or by the irradiation of strong X-rays [7, 8]. Recently, using scanning tunneling microscopy (STM), Kanasaki et al. have discovered that the irradiation of visible photons onto the graphite induces novel nanosize $sp^2 \rightarrow sp^3$ collective conversion [9, 10]. The STM image shows the nanosize domain in which 4 carbons in each six-membered ring rise up from the layer and residual 2 carbons sink down and approach the second layer, as shown in Fig. 1a. The sinking down carbons form interlayer σ bonds between the first and the second layers (Fig. 1b). Due to the AB stacking of the graphite, two types of interlayer bonded carbon pairs coexist, namely, α and β pairs. In order to stabilize these interlayer bonds, shear displacement occurs between the two layers. The resultant domain is stable for several days at room temperature.

In this photoinduced phenomenon which is quite different from the conventional graphite–diamond conversion, only a microscopic energy of several photons enough to nucleate a minimum kernel of the new phase is given to a local and limited area of a crystal. This minimum kernel will proliferate stepwise, according to the hidden stability intrinsic to the graphite. This kind of process is called a photoinduced structural phase transition [11–15]. The

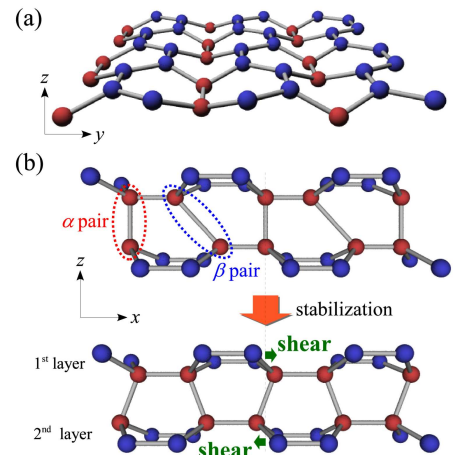


Fig. 1. The structure of diaphite. (a) The top-down view of the first layer. The blue spheres indicate rising up carbons from the layer and the red ones are sinking down carbons. (b) The side view of the diaphite. When the first and the second layers just approach each other, the interlayer bonds in β pairs are unstable (upper illustration). Therefore, the shear displacement occurs so that the diaphite structure is stabilized (lower illustration).

photoinduced nanosize domain shown in Fig. 1 is not the diamond, but an intermediate state between the graphite and the diamond, which is called “diaphite” [9, 10].

The adiabatic property of this phase transition has been studied by calculating the adiabatic path from the graphite to the small diaphite domain, by means of the lo-

cal density approximation (LDA) [16] and by the semiempirical Brenner theory [17, 18] which can describe various carbon cluster systems. Next, we have studied the early stage dynamics of the interlayer σ bond formation [18, 19]. As a result, we found that the self-localization of photoexcited electron–hole pair spanning two layers occurs within a few femtoseconds at the probability of about 2% when the electron–hole pair is excited as a transient state with the energy of 3.3 ± 1.8 eV. After the self-localization, by using a classical molecular dynamics (MD) with the Brenner potential, we obtained that the subsequent bond formation is achieved within about 0.5 ps when the excitation energy is more than 4.5 eV. Moreover, we investigated the effects of random multisite excitation [20]. Consequently, due to the cooperative phenomena between excited sites, the number of formed interlayer bonds increases nonlinearly with respect to the number of excited sites. This theoretical result is also confirmed qualitatively by the experiment [9].

However, the structure of the obtained domain with interlayer σ bonds is quite different from the diaphite. In our calculation, all the interlayer bonds have been formed only in α pairs (hereafter referred as α bonds), but not in β pairs (β bond) at all. As shown in Fig. 1b, the diaphite includes alternatively α and β bonds. Since the β bonds are unstable due to the AB stacking, they have not been formed in our calculation. As mentioned above, the β bonds are stabilized by the shear displacement between layers like the lower structure of Fig. 1b. Thus, the existence of the shear is particularly important for the formation of the diaphite domain, as already discussed in our previous works [9, 16–20]. Experimental investigations have already confirmed that the shear displacement is generated under fs laser irradiation [9, 21].

In this paper, using the MD, we investigate how β bonds are successfully formed. The main reason why no β bond is formed in our previous calculation is due to the absence of shear displacement in the initial state of the MD. The quantum and thermal fluctuations of various lattice motion, including shearing motion, must always exist everywhere in actual graphite systems. If a β pair is excited when transient shear displacement occurs so that the two carbons of the pair approach each other, a β bond is possible to be formed there, freezing the shear displacement around it. Therefore, we introduce the fluctuation of shear displacement to the initial state. As known well, a graphite crystal has a main E_{2g} mode at 1580 cm^{-1} , corresponding to the in-plane vibration mode of aromatic carbons [22]. For simplicity, we take into account the fluctuation only of this mode. We approximately take place the E_{2g} vibration to a classical and random fluctuation at 2273 K ($= 1580\text{ cm}^{-1}$). Under the situation where there is the fluctuation in the initial state, we perform the random multisite excitation and investigate the effect of the initial fluctuation on the β bond formation. In addition, we study the excitation under the existence of coherent shearing motion. In our previous work [20], we showed that transient and coherent shear occurred

after the graphite was excited. We investigate how an additive excitation generates β bonds, freezing the transient shear before it disappears, and propose a two-pulse laser-excitation for efficiently photoinducing a nanosize domain with frozen shear.

2. Theoretical method

We use a classical MD and a semiempirical Brenner potential [1] in all calculations. The system consists of two graphite layers with the initial interlayer distance 3.35 \AA , and each layer includes 6240 carbons in about $128\text{ \AA} \times 128\text{ \AA}$, wherein a periodic boundary condition is imposed. In order to get an initial state with the fluctuation corresponding to the in-plane vibration of 1580 cm^{-1} , we perform a constant temperature (NVT ensemble) MD with a Nose–Hoover algorithm [23] at 2273 K, restricting carbon atoms only to in-plane motion. Using the initial state, we perform the random multisite excitation for a certain excitation density, as well as in our previous work [20]. Here we assume that the interlayer distance contracts locally at several sites of the crystal due to the self-localization of photoexcited electron–hole pairs. Then, the two carbons spanning two layers at each excited site are intruded inside of the two layers and have a velocity toward the inside. That is, in our MD calculation, the energy of photoexcitations are replaced by the potential and kinetic energy of the two carbons [19]. Let us note that we use a microcanonical (NVE) ensemble MD for the dynamics from $t = 0$. We count out the number of α and β bonds at 1.0 ps. We repeat the similar calculation 50 times and average the results. By performing the calculations for various excitation densities, we investigate the density dependence on the number of these two types of bonds.

In the case of the excitation under coherent shear, we give the first excitation to the system with no initial fluctuation. After a certain period of time Δt passes from the first excitation which makes the coherent shear, we give an additive excitation to the system. The excitation density of the second excitation is the same as that of the first excitation, where we consider only 6% excitation which is enough to induce cooperative phenomena in the interlayer bond formation [20]. We count out the number of bonds at 1.0 ps after the second excitation. By performing the calculations for various values of the time interval Δt , we investigate the Δt dependence on the bond formation.

3. Results and discussion

3.1. Excitation under shear fluctuation

In Fig. 2, we show the three examples of the initial states obtained by NVT-MD at 2273 K, which are taken from the view over the graphite layers. The color on the graphite means the shear displacement of the upper layer relative to the lower one, and its magnitude and direction are represented by the circular color palette. As seen

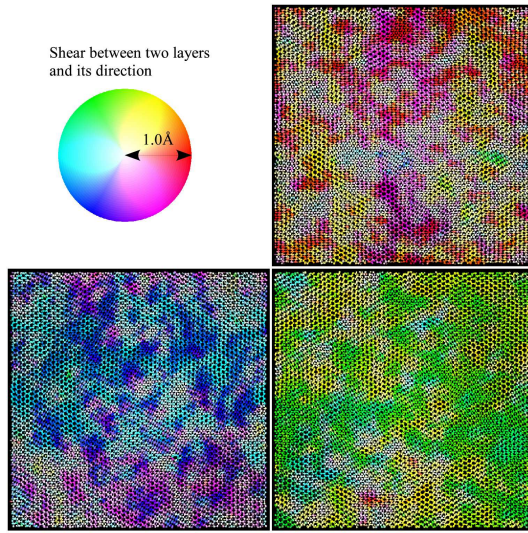


Fig. 2. Three examples of initial states obtained by NVT-MD at 2273 K. These are the top-down view of graphite layers and the color on the graphite means the shear between the upper layer and the lower one. Its magnitude and direction are represented by the circular color palette at the top left.

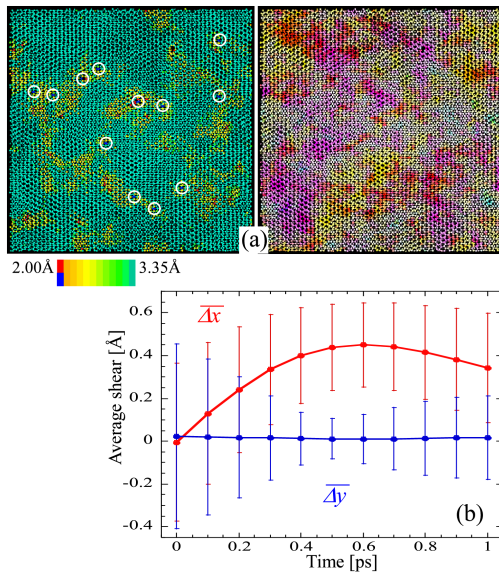


Fig. 3. (a) The snapshots of the MD calculation at $t = 1.0$ ps after the excitation of 10% density. The left figure indicates the interlayer distance represented by the color palette at the bottom, where red and blue denote α and β bonds, respectively. The β bonds are surrounded by white circles. The right figure is the shear displacement depicted in the same way as Fig. 2. (b) The average shear displacement in the case of the excitation density 10%, as a function of time. $\overline{\Delta x}$ and $\overline{\Delta y}$ are x and y components of the average shear, respectively.

from this figure, there are the shear fluctuations everywhere in every direction. Therefore, the average shear over all carbon sites and over 50 calculations is almost zero. Starting from these initial states, we perform the MD calculation for the random multisite excitation.

In Fig. 3a, as an example, we show the snapshots of the MD calculation at $t = 1.0$ ps in the case of the excitation density 10%, starting from the initial state at the top right in Fig. 2. The snapshot at the left side indicates the interlayer distance represented by the color palette at the bottom, where red and blue denote α and β bonds, respectively. The snapshot at the right side indicates the shear displacement depicted in the same way as Fig. 2. As seen from the snapshot of the interlayer distance at the left, several β bonds, which are surrounded by white circles for easiness to see, are formed. Moreover, as shown in the snapshot of the shear at the right, the color at the area including the β bonds remains red. This means that the shear does not disappear unless the β bonds are broken. In other words, the shear is frozen by the β bond formation. We can confirm this fact from Fig. 3b which shows the average shear displacement in the case of the excitation density 10%, as a function of time. $\overline{\Delta x}$ and $\overline{\Delta y}$ are x and y components of the average shear, respectively. Here we average the shear displacement for each carbon site over all sites and then average it over the number of calculations (= 50). After the excitation at $t = 0$, $\overline{\Delta x}$ increases gradually until about 0.6 ps, and then decreases. However the decrease is slower and $\overline{\Delta x}$ keeps enough large even at $t = 1.0$ ps. This indicates that a certain amount of the shear is frozen.

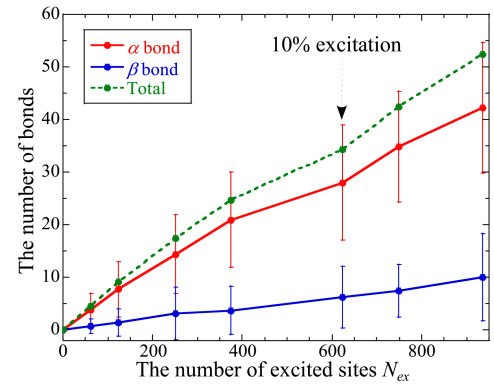


Fig. 4. The number of interlayer bonds counted at 1.0 ps, as a function of the number of excited sites N_{ex} . The red and blue solid lines indicate the number of α and β bonds, respectively, and the green dashed one is the sum of them.

We perform similar calculations for various excitation densities. Figure 4 shows the number of interlayer bonds, counted at 1.0 ps and averaged over 50 calculations, as a function of the number of excited sites. The red and blue solid lines indicate the number of α and β bonds, respectively, and the green dashed one is the sum of them. As seen from this figure, both the interlayer bonds in-

crease as the excitation density increases. The efficiency of the total interlayer bond formation is lower than that in the case without initial fluctuation [20], and hence cooperative phenomena do not appear enough to see the nonlinear increase of interlayer bonds. However, it is important that β bonds can be formed due to the shear fluctuation.

3.2. Excitation under coherent shear

Next, we consider the excitation under the transient and coherent shear. As mentioned above, in our previous calculation, such shearing motion occurs after the graphite is excited [20]. Figure 5 shows the average shear displacement in x direction as a function of time in the case of the excitation density 6%. The average shear seems to oscillate with a period of about 3.2 ps. Since the existence of the shear makes β bonds stable, they are expected to be formed easily when the graphite is excited again while the shear exists.

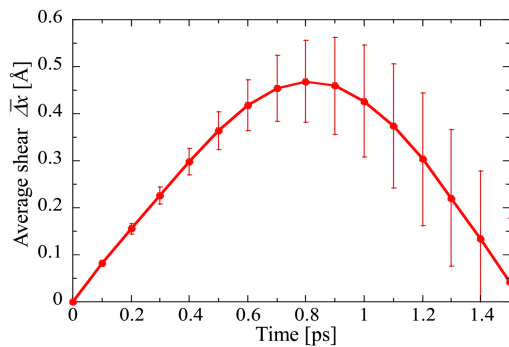


Fig. 5. The average shear displacement in x direction as a function of time. The 6% excitation is given to the system at $t = 0$. It is averaged over all carbon sites and over 50 calculations.

As an example, we show snapshots of the MD calculation for the case of $\Delta t = 0.4$ ps in Fig. 6. The upper two snapshots are taken at 0.4 ps after the first excitation, and the lower ones are at 1.0 ps after the additive excitation, where the left side snapshots indicate the interlayer distance, and the right side ones are the shear displacement. As seen from this figure, although there is almost no β bond at 0.4 ps after the first excitation, many β bonds are formed at 1.0 ps after the additive excitation. The β bonds tend to be formed near α bonds since the interlayer distance is contracting there. These interlayer bonds result in the small domains in which the interlayer distance is contracted. Moreover, as shown in the snapshot of the shear at the bottom right, the color of the domain including β bonds remains red, that is, the shear is frozen.

Figure 7 shows the Δt dependence on the number of interlayer bonds, where the meaning of the lines is the same as in Fig. 4. The values at $\Delta t = 0$ mean no additive excitation, corresponding to the 12% excitation only at once. For reference, the black rhombus at $\Delta t = 0$ indicates the number of α bonds for the 6% excitation at

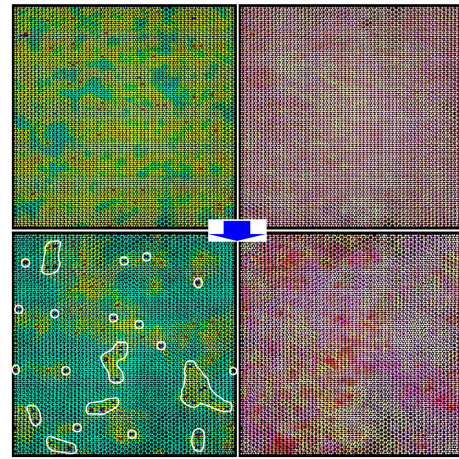


Fig. 6. The snapshots of the MD calculation at $t = 0.4$ ps after the first excitation (upper two snapshots) and at 1.0 ps after the second excitation (lower two snapshots) which is given to the system at $t = 0.4$ ps. The left side indicates the interlayer distance and the right side is the shear displacement. The domain including β bonds are surrounded by white curves.

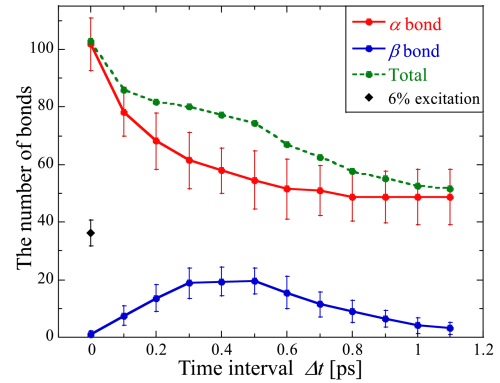


Fig. 7. The number of interlayer bonds counted at 1.0 ps after the second excitation, as a function of the time interval Δt between the first excitation and the second one. The values at $\Delta t = 0$ mean no additive excitation, corresponding to the 12% excitation only at once. The black rhombus at $\Delta t = 0$ corresponds to the 6% excitation only at once.

once. As seen from this figure, the number of α bonds monotonically decreases and settles down to a constant at more than $\Delta t = 0.9$ ps, while β bonds increase until $\Delta t = 0.5$ ps and afterward decreases gradually. In this calculation, the β bonds are formed most efficiently around $\Delta t = 0.3$ – 0.5 ps. In this time region, the average shear is increasing as seen from Fig. 5. Therefore, the excitation while the average shear increases is better for the β bond formation than the excitation at the maximum of the average shear at 0.8 ps. Although the number of β bonds remains lower than that of α bonds even in this region, it is essential that β bonds can be efficiently formed due to the coherent shear. Thus, we

propose the two-pulse excitation to achieve the efficient transition from the graphite to the diaphite.

4. Conclusion

We have studied theoretically the nonequilibrium formation process of sp^3 -bonded carbon nanodomains with frozen shear displacement between graphite layers by means of the MD calculation. We prepared the initial shear fluctuation corresponding to the 1580 cm^{-1} mode, and performed the random multisite excitation. As a result, we found that β bonds can be formed due to the shear fluctuation and the shear is frozen. Moreover, we investigated the excitation under the coherent shear by the two-pulse excitation. We found that the additive excitation can form β bonds efficiently due to the coherent shear generated by the first excitation. From these results, it is important for the interlayer bond formation with frozen shear that the shearing motion exists when the graphite is excited. If β bonds are formed once, the shear surrounding them remains stable. Through further excitation, new β bonds will be formed more easily around the existing shear. Therefore, β bonds will proliferate comparably to the proliferation of α bonds. As the number of these two types of bonds increases enough, the diaphite will be achieved.

Acknowledgments

This work is supported by the Ministry of Education, Culture, Sports, Science and Technology of Japan, the peta-computing project, and Grant-in-Aid for Scientific Research (S), contract No. 19001002, 2007.

References

- [1] D.W. Brenner, *Phys. Rev. B* **42**, 9458 (1990).
- [2] S. Fahy, S.G. Louie, M.L. Cohen, *Phys. Rev. B* **34**, 1191 (1986).

- [3] S. Fahy, S.G. Louie, M.L. Cohen, *Phys. Rev. B* **35**, 7623 (1987).
- [4] Y. Tateyama, T. Ogitsu, K. Kusakabe, S. Tsuneyuki, *Phys. Rev. B* **54**, 14994 (1996).
- [5] F. Bundy, *J. Chem. Phys.* **38**, 631 (1963).
- [6] T. Irifune, A. Kurio, S. Sakamoto, T. Inoue, H. Sumiya, *Nature (London)* **421**, 599 (2003).
- [7] F. Banhart, *J. Appl. Phys.* **81**, 3440 (1997).
- [8] H. Nakayama, H. Katayama-Yoshida, *J. Phys., Condens. Matter* **15**, R1077 (2003).
- [9] J. Kanasaki, E. Inami, K. Tanimura, H. Ohnishi, K. Nasu, *Phys. Rev. Lett.* **102**, 087402 (2009).
- [10] Research highlights, *Nature (London)* **458**, 129 (2009).
- [11] K. Nasu, *Rep. Prog. Phys.* **67**, 1607 (2004).
- [12] K. Nasu, *Photoinduced Phase Transitions*, World Sci., Singapore 2004.
- [13] K. Yonemitsu, K. Nasu, *Phys. Rep.* **465**, 1 (2008).
- [14] S. Koshihara, *J. Phys. Conf. Ser.* **148**, 01101 (2009), and other papers in this volume.
- [15] K. Nasu, *Eur. Phys. J. B* **75**, 415 (2010).
- [16] H. Ohnishi, K. Nasu, *Phys. Rev. B* **79**, 054111 (2009).
- [17] H. Ohnishi, K. Nasu, *Phys. Rev. B* **80**, 014112 (2009).
- [18] L. Radosinski, K. Nasu, T. Luty, A. Radosz, *Phys. Rev. B* **81**, 035417 (2010).
- [19] K. Nishioka, K. Nasu, *Phys. Rev. B* **80**, 235420 (2009).
- [20] K. Nishioka, K. Nasu, *Phys. Rev. B* **82**, 035440 (2010).
- [21] T. Mishina, K. Nitta, Y. Masumoto, *Phys. Rev. B* **62**, 2908 (2000).
- [22] F. Tuinstra, J.L. Koenig, *J. Chem. Phys.* **53**, 1126 (1970).
- [23] S. Nose, *J. Chem. Phys.* **81**, 511 (1984).